IEEE Access
Multidisciplinary | Rapid Review | Open Access Journal

Received November 21, 2019, accepted December 2, 2019, date of publication December 6, 2019,
date of current version December 23, 2019.

Digital Object Identifier 10.1109/ACCESS.2019.2958206

Improving the Performance of Low Voltage Networks by an Optimized Unbalance Operation of Three-Phase Distributed Generators

ADOLFO GASTALVER-RUBIO[1], ESTHER ROMERO-RAMOS[2], (Member, IEEE), AND JOSÉ MARÍA MAZA-ORTEGA[2], (Member, IEEE)

[1]Ingelectus, 41092 Sevilla, Spain
[2]Department of Electrical Engineering, Universidad de Sevilla, 41092 Sevilla, Spain

Corresponding author: Adolfo Gastalver-Rubio (agastalver@ingelectus.com)

This work was supported by the Spanish Ministry of Economy and Competitiveness under Grant ENE2014-54115-R and Grant ENE2017-84813-R.

ABSTRACT This work focuses on using the full potential of PV inverters in order to improve the efficiency of low voltage networks. More specifically, the independent per-phase control capability of PV three-phase four-wire inverters, which are able to inject different active and reactive powers in each phase, in order to reduce the system phase unbalance is considered. This new operational procedure is analyzed by raising an optimization problem which uses a very accurate modelling of European low voltage networks. The paper includes a comprehensive quantitative comparison of the proposed strategy with two state-of-the-art methodologies to highlight the obtained benefits. The achieved results evidence that the proposed independent per-phase control of three-phase PV inverters improves considerably the network performance contributing to increase the penetration of renewable energy sources.

INDEX TERMS Low voltage systems, minimization of unbalances, smart grid optimization, three-phase balancing photovoltaic inverters.

NOMENCLATURE

The following notation has been considered within the paper:

$\mathcal{D}$:	complex variable.
$\boldsymbol{\mathcal{D}}$:	vector of complex variables.
D:	RMS magnitude of a complex variable.
d:	real variable or parameter.
d:	vector of real variables or real functions.
i, j, k, l:	indexes associated to buses.
q:	index associated to each of the network phases (a, b, c) and the neutral n.
p:	index associated to each of the network phases (a, b, c) but excluding the neutral n.

I. INTRODUCTION

The so-called *European design* for planning low voltage (LV) distribution networks consists of a three-phase four-wire network supplying loads from the three-phase secondary distribution transformer connected to medium voltage (MV) level as shown in Fig. 1.

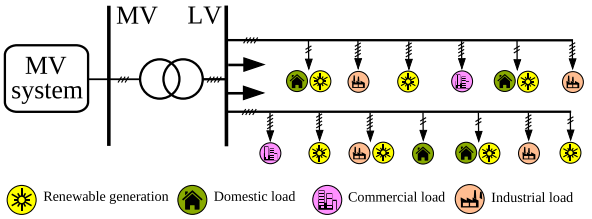

FIGURE 1. European design of LV distribution networks.

LV networks may have radial, ring or meshed structure, but are conventionally operated in a radial manner. This is the most extended layout used not only in Europe but also in other many countries all over the world [1]. One of the main power quality problems in these systems are the unbalances in voltage and more notably in currents. It is well-known that these unbalances are mainly caused by the unequal distribution of single-phase loads among the three phases, as well as the different consumption patterns of clients [2], [3]. These unbalances are getting worse because of the massive deployment of low-carbon technologies: distributed energy

The associate editor coordinating the review of this manuscript and approving it for publication was Yunfeng Wen.

resources (DERs), electric vehicles (EVs), battery energy storage systems (BESSs), etc. [4], [5]. Note that an unequal spread across the three phases of these single-phase devices may magnify unbalances. Worse still, the unbalances coming from these low-carbon technologies turn to be more significant than those coming from conventional loads because of their general higher power ratings and their long operation (charging or supplying energy) [6], [7]. In addition, the integration of these new technologies within the electrical installations of traditional consumers leads to the prosumer paradigm. This issue may have a large impact on the LV system unbalance because of the modifications of the conventional consumer daily profile which may lead to large demand variations, either increase or decrease, at different times of the day [8]. For all these reasons, some utilities have started to monitor their LV networks, confirming that voltage and current unbalances are greater than expected [9], [10].

Significant current unbalances can result in several problems, such as inefficient network utilization, higher losses, neutral and ground currents, neutral point-shifting, voltage outside statutory limits, voltage unbalances, etc. [8]. As a consequence, distribution system operators have been proposing different measures to mitigate these current unbalances at the LV side. Load balancing by manually switching the phase of each load [11] and adequate allocation of single-phase DER so they connect to the most convenient phase [12] have been explored. Other practical solutions consist on using static balancers for reducing neutral currents and voltage drops [8], [13]. More advanced dynamic measures, opposite to the previous static ones, have been proposed in the literature as those reported in [14] and [15], where the automation of controllable static switches is suggested in order to rearrange the connection of single-phase loads to the more suitable network phase. Recently, different authors have also proposed to use the three-phase inverters associated to DER, EV and BESS [16]–[21], being this measure quite promising thanks to the high operation flexibility of power electronic devices and their continuous lowering costs [22]. The additional functionalities provided by the inverters linked to the low-carbon technologies are well-known, although their use has been conventionally limited to their reactive power-based voltage control [12], [23]–[29]. Conversely, [30] proposes a double control by using not only the aforementioned reactive power capability but also real power curtailment of photovoltaic generators (PV) when needed. Moreover, a higher functionality can be achieved by adding an independent per-phase real power-based control. Resorting to this strategy, it should be possible to manage more power in one phase than in the others [16]–[21]. This possibility implies forgetting the common practice of only supplying a positive sequence current from the inverter and moving towards a more ambitious control, where the power converters are able to supply positive, negative and zero sequence currents [17]. The most appropriate power converter topologies able to implement these full power-based control are presented in [16], where fuel cell inverters are considered to compensate zero-sequence currents. The authors of [21] focus on the control strategies of DER inverters to optimize the voltage unbalance at the point of connection (POC) and at the point of common coupling (PCC). Also a local control mode for a three-phase DER inverter allocated at the PCC is presented in [18], looking for compensating downstream current unbalances. BESSs are considered in [19], where the authors analyze the controller influence on the BESS design intended for minimizing voltage unbalances and peak power of LV systems. The work conducted in [20] shows the improvements on the load balancing by using EV chargers and PV inverters whose operation is deduced by minimizing the sum of load variances of each phase.

This paper explores the impact that an independent per-phase control of three-phase inverters may have in the distribution system operation. Particularly, the objective is to use this advanced functionality to reduce the overall system unbalance as much as possible. For this reason, it is required to approach the problem from an utility perspective. This requires a precise LV network modelling and an optimization framework dealing with the unbalance minimization throughout the adequate independent per-phase power of three-phase inverters. To the knowledge of the authors, this problem has been never posed and solved before. Therefore, this paper can be envisioned as a technology scouting with the aim of assessing the role that this new operational mode may have in the distribution system. The paper just considers those three-phase inverters related to PV DERs due to its massive presence in distribution systems clearly prevailing over the rest of low-carbon technologies. The extrapolation to the use of three-phase inverters interfacing BESSs and EVs will be undertaken in a future research. In any case, this approach considers these new low-carbon technologies not as handicaps but as new resources able to bring several benefits to the system operation. This paper deeply analyzes this issue to facilitate the decision making of utilities about the massive deployment of this advanced per-phase independent control.

The paper is organized as follows: section II focuses on developing the electrical model considered for each of the components of the studied system, while section III presents the mathematical model of the optimization problem to solve. Section IV contanins the results obtained for a characteristic LV system under different simulation scenarios, showing the improvement level obtained at each case. Final conclusions are summarized in section V.

II. NETWORK MODELLING

This section is devoted to define the mathematical model of all those components within the European network arrangement shown in Fig. 1. Fig. 2 clarifies the adopted notation and allows to specify mathematically the working variables. The shunt elements in Fig. 2 can be either loads (L), PVs (denoted by 1G or 3G in case of single-phase or three-phase inverters respectively) or the equivalent MV system. The series elements refer to the branches between two nodes of the LV system or the coupling MV/LV transformer. The considered

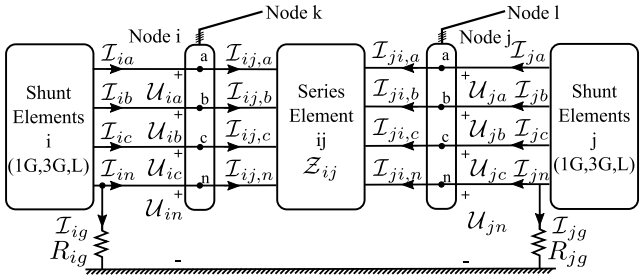

FIGURE 2. Detailed scheme of three-phase buses and variables.

LV system comprises $N+1$ nodes and N branches because of the network radiality. The main working variables are:

- Complex phase-to-ground voltage at node i: $\boldsymbol{\mathcal{U}}_i^T = [\mathcal{U}_{iq}]^T = [\mathcal{U}_{ia}\ \mathcal{U}_{ib}\ \mathcal{U}_{ic}\ \mathcal{U}_{in}]^T$.
- Complex phase current of different shunt components connected to node i: load current, $\boldsymbol{\mathcal{I}}_i^L$, DER current, $\boldsymbol{\mathcal{I}}_i^{1G}$ or $\boldsymbol{\mathcal{I}}_i^{3G}$, and ground resistor current $\mathcal{I}_{ig}$.
- Complex net phase current injection at node i: $\boldsymbol{\mathcal{I}}_i^T = [\mathcal{I}_{iq}]^T = [\mathcal{I}_{ia}\ \mathcal{I}_{ib}\ \mathcal{I}_{ic}\ \mathcal{I}_{in}]^T$.
- Complex phase current coming into node M from MV system: $\boldsymbol{\mathcal{I}}_M^T = [\mathcal{I}_{Mp}]^T = [\mathcal{I}_{Ma}\ \mathcal{I}_{Mb}\ \mathcal{I}_{Mc}]^T$.
- Complex phase current flow through the series branch ij: $\boldsymbol{\mathcal{I}}_{ij}^T = [\mathcal{I}_{ij,q}]^T = [\mathcal{I}_{ij,a}\ \mathcal{I}_{ij,b}\ \mathcal{I}_{ij,c}\ \mathcal{I}_{ij,n}]^T$.

Next subsections define the network equations and develop the model equations for each network component: MV system, secondary distribution transformer, three-phase four-wire lines, loads, PV generators and grounding resistors. In what follows rectangular coordinates are considered for any complex variable, and polar coordinates are just used in some cases for illustrative purposes only.

A. MEDIUM VOLTAGE SYSTEM

The MV system is modeled as a real voltage source by using a three-phase Thévenin equivalent. A grounded wye three-phase balanced ideal voltage source $\boldsymbol{\mathcal{E}}_M^T = [E\angle 0\ \ E\angle -120\ \ E\angle 120\ \ 0]^T$ with a series impedance $\mathcal{Z}_M$ is used by considering the actual operation voltage and the MV positive sequence short-circuit impedance respectively. This impedance $\mathcal{Z}_M$ is computed from the nominal voltage, the three-phase short-circuit power and the R/X ratio. Usual European grid equivalent data for MV networks are provided in [31] with short-circuit powers between 10 and 1000 MVA while R/X ratios varies from 0.4 to 2. This Thévenin equivalent allows to formulate the MV system model as follows:

$$\begin{bmatrix}\mathcal{U}_{Ma}\\ \mathcal{U}_{Mb}\\ \mathcal{U}_{Mc}\end{bmatrix} = \begin{bmatrix}E\angle 0\\ E\angle -120\\ E\angle 120\end{bmatrix} - \begin{bmatrix}\mathcal{Z}_M & 0 & 0\\ 0 & \mathcal{Z}_M & 0\\ 0 & 0 & \mathcal{Z}_M\end{bmatrix}\begin{bmatrix}\mathcal{I}_{Ma}\\ \mathcal{I}_{Mb}\\ \mathcal{I}_{Mc}\end{bmatrix}. \quad (1)$$

B. DISTRIBUTION TRANSFORMERS

The three-phase MV/LV transformer at the head of the system (see Fig. 1) is used to reduce the voltage for supplying the final users in a suitable way. The delta-grounded star connection with off-load tap changer is the most used transformer configuration in these secondary substations of European distribution systems [3].

Three-phase transformer models using a bus admittance matrix have been already proposed in the literature for all the possible connections, considering their primary and secondary taps and formulated either in per unit or actual values [32]–[35]. Special care is needed when the wye side of the transformer is grounded by using a finite resistor instead of a solidly grounded connection.

As an example, if a delta-grounded star configuration Dyn11 is considered for the three-phase MV/LV transformer, the resulting electrical model is defined by (2) and (3), as shown at the bottom of this page,

$$\mathcal{U}_{Ln} = R_{Lg}\left(\mathcal{I}_{LM,a} + \mathcal{I}_{LM,b} + \mathcal{I}_{LM,c} + \mathcal{I}_{LM,n}\right) \quad (2)$$

$$\begin{bmatrix}\mathcal{I}_{ML,a}\\ \mathcal{I}_{ML,b}\\ \mathcal{I}_{ML,c}\\ \hline \mathcal{I}_{LM,a}\\ \mathcal{I}_{LM,b}\\ \mathcal{I}_{LM,c}\end{bmatrix} = \left[\begin{array}{ccc|ccc} \frac{2\mathcal{Y}_{cc}}{\alpha^2} & -\frac{\mathcal{Y}_{cc}}{\alpha^2} & -\frac{\mathcal{Y}_{cc}}{\alpha^2} & -\frac{t\mathcal{Y}_{cc}}{\alpha\beta} & 0 & \frac{t\mathcal{Y}_{cc}}{\alpha\beta}\\ -\frac{\mathcal{Y}_{cc}}{\alpha^2} & \frac{2\mathcal{Y}_{cc}}{\alpha^2} & -\frac{\mathcal{Y}_{cc}}{\alpha^2} & \frac{t\mathcal{Y}_{cc}}{\alpha\beta} & -\frac{t\mathcal{Y}_{cc}}{\alpha\beta} & 0\\ -\frac{\mathcal{Y}_{cc}}{\alpha^2} & -\frac{\mathcal{Y}_{cc}}{\alpha^2} & \frac{2\mathcal{Y}_{cc}}{\alpha^2} & 0 & \frac{t\mathcal{Y}_{cc}}{\alpha\beta} & -\frac{t\mathcal{Y}_{cc}}{\alpha\beta}\\ \hline -\frac{t\mathcal{Y}_{cc}}{\alpha\beta} & \frac{t\mathcal{Y}_{cc}}{\alpha\beta} & 0 & \frac{t^2\mathcal{Y}_{cc}}{\beta^2} & 0 & 0\\ 0 & -\frac{t\mathcal{Y}_{cc}}{\alpha\beta} & \frac{t\mathcal{Y}_{cc}}{\alpha\beta} & 0 & \frac{t^2\mathcal{Y}_{cc}}{\beta^2} & 0\\ \frac{t\mathcal{Y}_{cc}}{\alpha\beta} & 0 & -\frac{t\mathcal{Y}_{cc}}{\alpha\beta} & 0 & 0 & \frac{t^2\mathcal{Y}_{cc}}{\beta^2} \end{array}\right] \begin{bmatrix}\mathcal{U}_{Ma}\\ \mathcal{U}_{Mb}\\ \mathcal{U}_{Mc}\\ \hline \mathcal{U}_{La}-\mathcal{U}_{Ln}\\ \mathcal{U}_{Lb}-\mathcal{U}_{Ln}\\ \mathcal{U}_{Lc}-\mathcal{U}_{Ln}\end{bmatrix} \quad (3)$$

$$\boldsymbol{\mathcal{U}}_i = \boldsymbol{\mathcal{Z}}_{ij}\boldsymbol{\mathcal{I}}_{ij} + \boldsymbol{\mathcal{U}}_j \rightarrow \begin{bmatrix}\mathcal{U}_{ia}\\ \mathcal{U}_{ib}\\ \mathcal{U}_{ic}\\ \mathcal{U}_{in}\end{bmatrix} = \begin{bmatrix}\mathcal{Z}_{ij,aa} & \mathcal{Z}_{ij,ab} & \mathcal{Z}_{ij,ac} & \mathcal{Z}_{ij,an}\\ \mathcal{Z}_{ij,ab} & \mathcal{Z}_{ij,bb} & \mathcal{Z}_{ij,bc} & \mathcal{Z}_{ij,bn}\\ \mathcal{Z}_{ij,ac} & \mathcal{Z}_{ij,bc} & \mathcal{Z}_{ij,cc} & \mathcal{Z}_{ij,cn}\\ \mathcal{Z}_{ij,an} & \mathcal{Z}_{ij,bn} & \mathcal{Z}_{ij,cn} & \mathcal{Z}_{ij,nn}\end{bmatrix}\begin{bmatrix}\mathcal{I}_{ij,a}\\ \mathcal{I}_{ij,b}\\ \mathcal{I}_{ij,c}\\ \mathcal{I}_{ij,n}\end{bmatrix} + \begin{bmatrix}\mathcal{U}_{ja}\\ \mathcal{U}_{jb}\\ \mathcal{U}_{jc}\\ \mathcal{U}_{jn}\end{bmatrix} \quad (4)$$

where indexes M, L are the MV and LV transformer nodes; t is the real transformer ratio; α and β are the tap positions at the primary and secondary sides with respect to their nominal values respectively; $\mathcal{Y}_{cc}$ is the rated short-circuit admittance referred to the MV primary side in Siemens with taps in the central rated position; and R_{Lg} is the ground resistor at the LV side of the transformer connecting its neutral with ground.

C. LOW VOLTAGE LINES

A variable number of feeders are supplied by the transformer, being these feeders usually underground or overhead cables, much less overhead lines [36]. Three-phase four-wire distribution lines are the most common configuration for LV branches, although single-phase sections are also identified to supply single-phase clients [3]. The modeling of overhead and underground line segments must be as precise as possible since this model plays an important role in the final solution [37]. The greater the load unbalances, the larger the inaccuracy because of the lack of precision in the modelling of lines [38].

Carson's equations allow to determine the phase series impedance matrix associated to any n-conductor line by taking into account its actual phasing and the correct spacing between conductors. A 4×4 series impedance matrix $\mathcal{Z}_{ij}$ results from the formulation (4), as shown at the bottom of the previous page, where $\mathcal{I}_{ij,m}$ denotes the current flow through the phase m of the line ij. Note that the series impedance matrix is completely full for a three-phase four-wire line and with only null elements for two-phase or single-phase lines.

D. LOAD MODELS

Most of loads connected to LV systems are single phase, although three-phase consumers are also connected. Three-phase loads can be configured either in delta or wye connections, while single-phase loads connect between a phase and neutral or scarcely between two phases.

For steady-state analysis, the voltage dependency of load models needs to be specified. Generally, loads are grouped in three categories (ZIP model): constant power loads (power demand is constant regardless of the voltage), constant current loads (power demand is proportional to the voltage), or constant impedance loads (power demand is proportional to the voltage squared). The most widely used model in static studies is the constant power model because a safer evaluation of voltage profiles is obtained [39], [40]. For this reason, constant power model has been considered although any other model can be easily implemented. As an example, the model of a wye load L connected to bus i is defined as:

$$\boldsymbol{\mathcal{S}}_i^L = \begin{bmatrix} \mathcal{S}_{ia}^L \\ \mathcal{S}_{ib}^L \\ \mathcal{S}_{ic}^L \end{bmatrix} = \begin{bmatrix} (\mathcal{U}_{ia} - \mathcal{U}_{in})(\mathcal{I}_{ia}^L)^* \\ (\mathcal{U}_{ib} - \mathcal{U}_{in})(\mathcal{I}_{ib}^L)^* \\ (\mathcal{U}_{ic} - \mathcal{U}_{in})(\mathcal{I}_{ic}^L)^* \end{bmatrix}, \tag{5}$$

$$\mathcal{I}_{ia}^L + \mathcal{I}_{ib}^L + \mathcal{I}_{ic}^L + \mathcal{I}_{in}^L = 0 \ . \tag{6}$$

where $\mathcal{S}_{ip}^L$ denotes the injected power at each phase p. The model for a delta-connected load can be easily deduced in a similar way, but it has not been included due to space limitations. For both connections, either wye or delta, the same phase power has to be considered if a balanced three-phase load is modeled: $\mathcal{S}_{ia}^L = \mathcal{S}_{ib}^L = \mathcal{S}_{ic}^L$. Otherwise, in case of a single-phase load, the corresponding missing phase currents are set to zero.

E. PV GENERATORS

PV generators integrated in the LV network may have either a single-phase or a three-phase connection mainly depending on their rated power. In any case, and irrespectively of their connection, PV generators are modeled as constant power injections $\boldsymbol{\mathcal{S}}_i^G$ in a similar way than the load model. Regarding the active power, PV generators are assumed to operate injecting the maximum available power which varies depending on the irradiance. Likewise, reactive power injection can be set depending on the standing grid code, being unity power factor operation a common practice for PV generators connected to LV networks. Single-phase generators connected to a phase p and the neutral n of the bus i are modelled as:

$$\mathcal{S}_{ip}^{1G} = \mathcal{U}_{ip}(\mathcal{I}_{ip}^{1G})^*, \quad \mathcal{I}_{ip}^{1G} + \mathcal{I}_{in}^{1G} = 0. \tag{7}$$

The contribution of the paper lies on assessing the benefits of an independent per-phase operation of the three-phase PV generators for optimizing the performance of the LV network in terms of power loss minimization. Obviously, this operational mode strongly depends on the PV inverter topology being possible to find in the specialized literature the following cases [41]:

- Three-phase three-wire inverter. The operational constraint of this topology, shown in Fig. 3.a, is that the sum of the phase currents must be equal to zero:

$$\mathcal{I}_{ia}^{3G} + \mathcal{I}_{ib}^{3G} + \mathcal{I}_{ic}^{3G} = 0. \tag{8}$$

  Therefore, it is not possible to inject any zero sequence current being the unbalance operation limited to negative sequences.
- Three-phase four-wire inverter. In this case, the additional neutral wire adds a degree of freedom to the inverter operation being possible to inject zero sequence currents. The operational constraint can be formulated in this way:

$$\mathcal{I}_{ia}^{3G} + \mathcal{I}_{ib}^{3G} + \mathcal{I}_{ic}^{3G} + \mathcal{I}_{in}^{3G} = 0. \tag{9}$$

  Note that the topology shown in Fig. 3.b is one of the proposed for this type of three-phase four-wire inverters but many other alternative topologies can be found in [42], [43]. Additionally, this three-phase four-wire configuration could be also achieved by merging single-phase units connected between the different phases and the neutral wires and sharing a common DC bus as shown in Fig. 3.c [44].

This review of already existing three-phase inverter topologies highlights the technology readiness which allows to

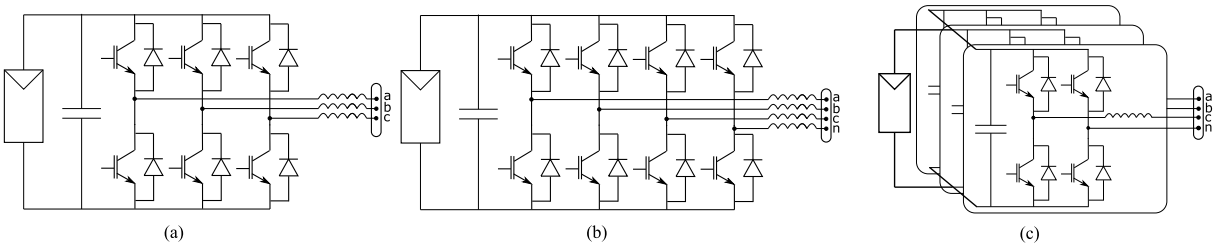

FIGURE 3. Three-phase inverter topologies. (a) Three-wire inverter. (b) Four-wire inverter. (c) Set of single-phase inverters.

apply the proposed independent per-phase control of active and reactive power.

Two more constraints have to be applied to the operation of three-phase inverters. Firstly, the injected power has to be equal to the available power P_i^{3G} which mainly depends on the irradiance:

$$\Re\left(\left(\mathcal{U}_{ia}-\mathcal{U}_{in}\right)\left(\mathcal{I}_{ia}^{3G}\right)^{*}+\left(\mathcal{U}_{ib}-\mathcal{U}_{in}\right)\left(\mathcal{I}_{ib}^{3G}\right)^{*} + +\left(\mathcal{U}_{ic}-\mathcal{U}_{in}\right)\left(\mathcal{I}_{ic}^{3G}\right)^{*}\right)=P_i^{3G}. \quad (10)$$

This equation turns into a less than or equal to inequality when curtailment is allowed. Secondly, inverter capacity has to be considered. In this sense, it is quite common oversizing PV inverters with respect to the ones operating with unity power factor because they offer reactive power support to comply with the requirements imposed by the existing grid codes [45], [46]. Since this paper proposes an unbalanced control of three-phase PV inverters involving an independent per-phase control of the active and reactive power, it is expected that the PV inverter has to be oversized. As a result, the phase current of a PV inverter, I_{ip}^{3G}, has to be always below the maximum current, $I_i^{3G,max}$, which is oversized by a factor ρ_i with respect to the maximum current of balance operation:

$$\left(I_{ip}^{3G}\right)^2 \le \left(I_i^{3G,max}\right)^2 = \rho_i^2\left(\frac{S_i^{3G,nom}}{\sqrt{3}U_i^{3G,nom}}\right)^2, \quad (11)$$

where the superscript *nom* refers to nominal values. Note that the constraint (11) has been formulated in a quadratic form to avoid the square roots required for computing the RMS value of a complex magnitude represented by rectangular coordinates. In this way, the strong non-linearity introduced by the square root in the optimization problem is eliminated.

F. GROUNDING RESISTORS

The LV network grounding depends on regional preferences. Mostly, the LV networks are directly earthed at the star point of the MV/LV transformer, while the neutral wire is grounded at multiple points along the network through resistors because of safety issues. The values of these resistors depend on the type of earth electrode, the earth conductor and the terrain resistivity. These characteristics determine the value of the final resistor R_{ig} to be considered at each bus i, that theoretically is within the interval between zero and infinity. The current flowing through the ground resistor $\mathcal{I}_{ig}$ can be formulated as:

$$\mathcal{I}_{ig}=\begin{cases}\dfrac{\mathcal{U}_{ig}}{R_{ig}} & \text{if } R_{ig}\neq\infty\\ 0 & \text{if } R_{ig}=\infty.\end{cases} \quad (12)$$

G. NETWORK EQUATIONS

Kirchhoff's laws have to be enforced considering the existing network topology. Kirchhoff's voltage law has been already taken into account through the formulation of the transformer and line models (3) and (4) respectively. Therefore, no additional equations are needed because of the network radiality.

The systematic formulation of Kirchhoff's current laws is based on the node incidence matrix $\mathbf{A}$, associated to the oriented-type graph describing the system topology. The number of rows of $\mathbf{A}$ is equal to the number of series branches multiplied by 4, because of the LV system is a four-wire network, and the number of columns is four times the number of buses:

$$\mathbf{A}\left[\mathcal{I}_{ij,q}\right]=\left[\mathcal{I}_{kq}\right]. \quad (13)$$

The net current injection coming into bus k through phase q $[\mathcal{I}_{kq}]$ is a function of all the currents flowing through the different shunt components connected to this bus such as loads, PV generators and grounding resistors:

$$\mathcal{I}_{kp}=\sum_{L,1G,3G\in k}\left(\mathcal{I}_{kp}^{L}+\mathcal{I}_{kp}^{1G}+\mathcal{I}_{kp}^{3G}\right), \quad (14)$$

$$\mathcal{I}_{kn}=\sum_{L,1G,3G,R_{kg}\in k}\left(\mathcal{I}_{kn}^{L}+\mathcal{I}_{kn}^{1G}+\mathcal{I}_{kn}^{3G}-\mathcal{I}_{kg}\right). \quad (15)$$

III. OPTIMIZATION PROBLEM

Any optimization problem minimizes or maximizes an objective function f subject to a set of equality $\mathbf{g}$ and/or inequality $\mathbf{h}$ constraints which can be formulated as follows:

$$\begin{aligned}&\min f(\mathbf{x},\mathbf{u})\\ &\text{s.t. } \mathbf{g}(\mathbf{x},\mathbf{u})=0\\ &\quad \mathbf{h}(\mathbf{x},\mathbf{u})\le 0.\end{aligned} \quad (16)$$

where vector $\mathbf{x}$ comprises the dependent or state variables and vector $\mathbf{u}$ the control variables of the problem. For the posed problem, complex phase currents injected by PV inverters, $\mathcal{I}_i^{3G}$, make up the control vector $\mathbf{u}$, while the vector $\mathbf{x}$ is composed by the nodal voltages and the rest of currents required to

model the system components. Following a detailed description of the objective function and the equality and inequality constraints is included.

It is known that a balanced three-phase power system, both in design (symmetric network impedances) and operation (balanced load and generation), presents the best performance in terms of power losses. Any unbalance perturbation from this optimal configuration implies an increase in losses. Since this work is mainly aimed in reducing unbalances, a way of reaching this objective consists of minimizing active power losses. Power losses of the three-phase four-wire system under analysis can be easily obtained by setting out the power balance of the system as:

$$\mathcal{S}_{loss} = \mathcal{U}_M^T \mathcal{I}_M^* + \sum_{i}^{N+1} \sum_{p} \left[\mathcal{S}_{ip}^G - \mathcal{S}_{ip}^L \right]. \tag{17}$$

Active power losses correspond to the real part of (17), so the objective function of the optimization problem results:

$$f(\mathbf{x}, \mathbf{u}) = \Re(\mathcal{S}_{loss}). \tag{18}$$

Regarding the equality and inequality constraints, **g** and **h**, these are formed by all the equations defined in section II, remaining only to include those inequalities due to operational constraints. To enable an efficient and secure system performance, it is required to consider the operational limits of all the series system components in terms of voltage and currents. The thermal capacity of any series element ij is considered as follows:

$$\left(I_{ij,q}\right)^2 \leq \left(I_{ij,q}^{max}\right)^2, \tag{19}$$

where $I_{ij,q}^{max}$ denotes the maximum current through each phase q of a branch ij. Just like in (11), squared currents are considered to obtain a more linear set of equations. Similarly, any phase nodal voltage, $\mathcal{U}_{ip} - \mathcal{U}_{in}$, has to be within the regulatory limits:

$$\left(U^{min}\right)^2 \leq \left(\mathcal{U}_{ip} - \mathcal{U}_{in}\right)\left(\mathcal{U}_{ip} - \mathcal{U}_{in}\right)^* \leq \left(U^{max}\right)^2. \tag{20}$$

Summarizing, the final optimization problem to solve is:

$$\begin{aligned} &\min\ \Re(\mathcal{S}_{loss}) \\ &\text{s.t. Equality constraints } \mathbf{g}: \\ &\quad \begin{bmatrix} \text{MV system: (1)} \\ \text{Distribution transformer: (2), (3)} \\ \text{Low voltage lines: (4)} \\ \text{Loads: (5), (6)} \\ \text{PVs: (7), (10) and (8) or (9)} \\ \text{Grounding resistors: (12)} \\ \text{Network equations: (13), (14), (15)} \end{bmatrix} \\ &\quad \text{Inequality constraints } \mathbf{h}: \\ &\quad \begin{bmatrix} \text{PV oversizing: (11)} \\ \text{Operational constraints: (19), (20)} \end{bmatrix}. \end{aligned} \tag{21}$$

The final optimization problem (21) is a nonlinear non-convex static programming problem with continuous variables. Interior-point method is an attractive approach to solve it in comparison to other classical methodologies (gradient methods, sequential quadratic programming, Karush-Kuhn Tucker optimality conditions, etc). Convergence speed and ability to manage inequality constraints are two of the more relevant advantages of interior-point methods [47]. The primal-dual interior-point algorithm is the considered throughout this work [48]. It is not the objective of this paper to analyze convexity, smoothness, continuity and differentiability of (21), although the posed problem is very close to the well-known *Optimal Power Flow* (OPF) for the operation of power systems, for which interior-points methodologies have proved to be quite efficient [47]. Note that all variables in (21) are continuous, so the considered optimization problem is even easier than classical OPFs where discrete variables make worse the aforementioned mathematical properties. Finally, it is important to remark that the optimization problem has been formulated in the complex phase domain but a final transformation to the corresponding two equivalent real equations is required, this step being omitted for the sake of brevity.

IV. SIMULATION RESULTS

This section is devoted to analyze the proposed unbalanced operation of three-phase PV inverters for balancing the LV distribution grid. This is done by running hourly scenarios during a day using the CIGRE Task Force C06.04.02 LV European benchmark system [31]. To clearly assess the benefits of the proposal, a comparison with traditional operational strategies throughout different scenarios is carried out. This comparison is performed by means of a comprehensive set of representative key performance indexes (KPIs).

A. BENCHMARK NETWORK

The standard three-phase four-wire distribution LV European benchmark network proposed in [31] has been slightly modified to include just the residential feeder with a 300 MVA MV/LV transformer as shown in Fig. 4 ($\mathcal{Z}_{cc} = 0.0053 + 0.0213j\ \Omega$ refered to secondary side, $R_{1g} = 3\ \Omega$). DER units are connected within the node set $G = \{R2, R15, R18\}$. The 24-hour total and per-phase active and reactive power profiles of load and PV generation are shown in Fig. 5.

B. SCENARIO PARAMETERS

In order to study the performance of the control strategies in different scenarios, combinations of the following parameters are considered:

- Percentage of renewable generation with respect to the maximum load power consumption $\sigma \in [0, 2]\,pu$. The DER generation in this network is PV, thus, in the largest σ scenario, the overall network will generate active power to the grid at the hours close to the point of maximum solar irradiance.
- Percentage of presence of three-phase four-wire generation $\tau \in [0, 1]\,pu$. The larger this parameter, the more controllable unbalance three-phase four-wire inverters

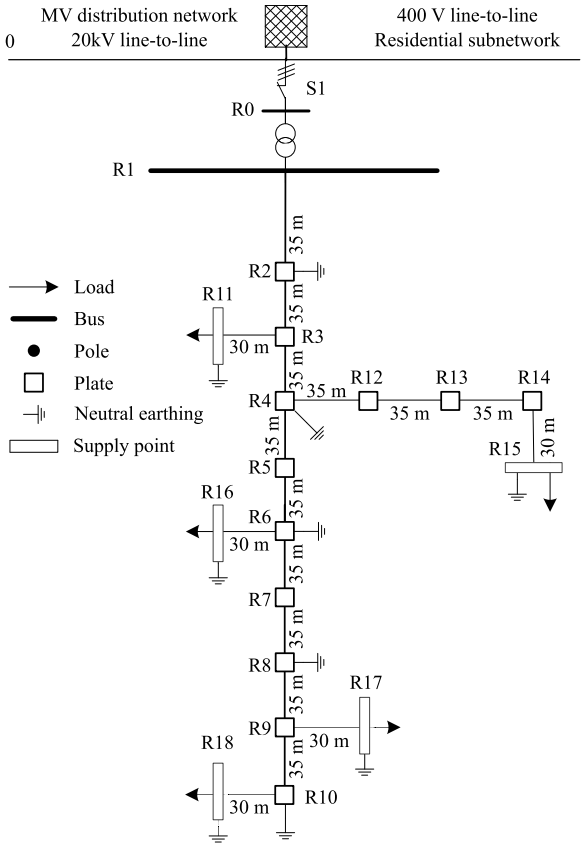

FIGURE 4. CIGRE Task Force C06.04.02 European LV benchmark network (residential feeder) [31].

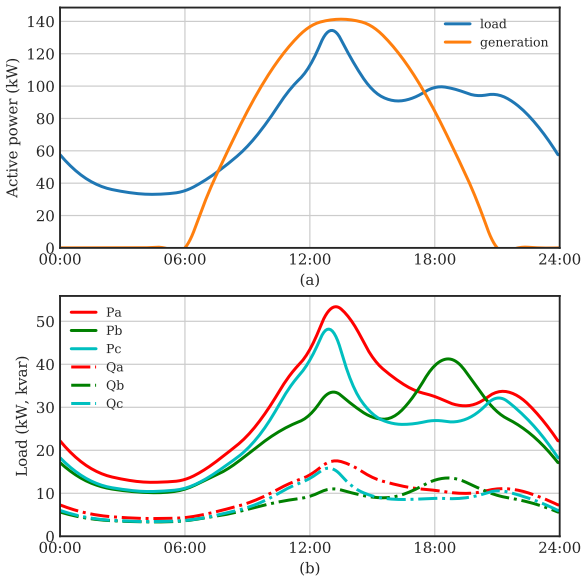

FIGURE 5. Daily load and generation active and reactive power profiles: (a) Aggregated total active power. (b) Aggregated per-phase active and reactive load powers.

able to contribute to the network balancing. The single-phase PV units are distributed equally between the three phases as planning engineers commonly do with new loads, trying to balance the system as much as possible.

- Photovoltaic inverter oversizing ratio $\rho \in [1, 3]\,pu$, previously introduced in (11).

C. CONTROL STRATEGIES

In order to highlight the benefits of the proposal, which is based on an unbalanced operation of the active and reactive power injected by PV inverters, a comparison with other two conventional operating strategies is performed. In the first strategy the PV inverters just inject active power with an unity power factor which is quite common for this type of generation connected to LV networks. The second strategy takes advantage of the reactive power capability of PV inverters for minimizing the system power losses. In this last case it is solved an optimization problem similar to (21) but considering the classical balanced operation of the three-phase PV inverters. In summary, three strategies of operation are tested $\zeta \in \{bc, bal, unbal\}$, where *bc* refers to the base case with PV inverters operating at unity power factor (non-optimized operation), *bal* refers to the optimal balanced control of reactive power and *unbal* is used to refer to the proposed optimal unbalanced control strategy. Therefore, the comparison of the two optimal control strategies with respect to the base case will highlight the benefits of the proposed independent per-phase control of DERs. It has to be pointed out that the control strategies do not include curtailment to establish a fair comparison among them. In this sense, a modified objective function would be required to penalize those solutions which use the curtailment as a resource to optimize the distribution system operation.

D. KEY PERFORMANCE INDICATORS

Let $\Re(\mathcal{S}_{loss})_h^\zeta$ be the objective function value after performing the operation strategy ζ at the hour h. For each of these solutions ζ, the LV distribution network is operating with a voltage profile $(\mathcal{U}_{iq})_h^\zeta$ for the phase q, node i at the hour h. Considering this, the following KPIs can be defined to quantify the benefits of the proposal:

- Losses reduction. The percentage of losses of the strategy ζ with respect to the non-optimized operation strategy ($\zeta = bc$), $\mathbb{KPI}_{loss}^\zeta$, is defined as an indicator of efficiency:

$$\mathbb{KPI}_{loss}^\zeta = \frac{\sum_{h=0}^{23} \Re(\mathcal{S}_{loss})_h^\zeta}{\sum_{h=0}^{23} \Re(\mathcal{S}_{loss})_h^{bc}}. \tag{22}$$

  The lower this index, the higher the efficiency of the optimized operation of the system.
- Network voltage range. This index measures the maximum hourly range of the network phase nodal voltages in per unit with respect to the rated voltage and for each control strategy ζ:

$$\mathbb{KPI}_{\Delta V,h}^\zeta = \frac{\max\limits_{i,p} |\mathcal{U}_{ip,h} - \mathcal{U}_{in,h}| - \min\limits_{j,p} |\mathcal{U}_{jp,h} - \mathcal{U}_{jn,h}|}{V_{nom}}. \tag{23}$$

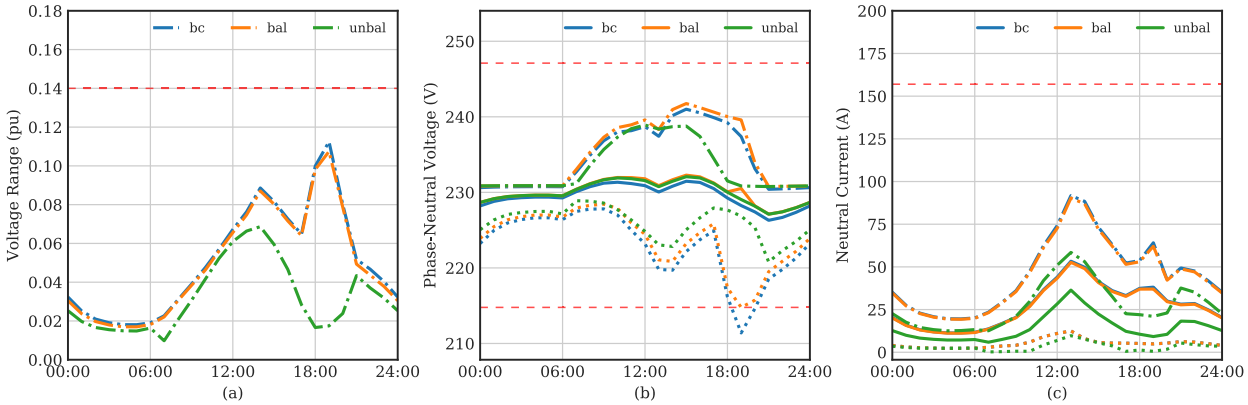

FIGURE 6. Daily evolution of (a) $\mathbb{KPI}^{\zeta}_{\Delta V,h}$, (b) Phase-neutral voltages, (c) $\left|\mathcal{I}_{ij,n}\right|$. Maximum values (dash-dotted lines), average values (continuous line), minimum values (dotted line).

The sub-index h is added to $\mathcal{U}_{ip}$ and $\mathcal{U}_{jn}$ to indicate the value at the hour h of the day. It is important to point out that this index is not the nodal voltage range, i.e. the difference between the maximum and the minimum voltage of a given node. As a consequence, this KPI provides a global information about the network voltages. A low value of this index implies a narrow voltage variation of the network nodal voltages.

- Maximum voltage unbalance. This KPI indicates the maximum value of the voltage unbalance factor, VUF, of the control strategy ζ for a given hourly scenario. This indicator is again defined for nodal voltages:

$$\mathbb{KPI}^{\zeta}_{VUF0,h} = \max_i \left|\frac{\mathcal{U}_{0i,h}}{\mathcal{U}_{1i,h}}\right|$$
$$\mathbb{KPI}^{\zeta}_{VUF2,h} = \max_i \left|\frac{\mathcal{U}_{2i,h}}{\mathcal{U}_{1i,h}}\right|. \quad (24)$$

  where $\mathcal{U}_{0i,h}$, $\mathcal{U}_{1i,h}$ and $\mathcal{U}_{2i,h}$ refer to the symmetrical components of phase nodal voltages at bus i at hour h.
- Violations of voltage limits. This $\mathbb{KPI}^{\zeta}_{viol}$ is defined as the number of hours where the voltage regulation limits imposed by the standards are not met. The nodal voltage range and the inverse component voltage unbalance are limited to $\pm 7\%$ and 2% respectively according to the Spanish regulation [50] and [49]
- Maximum neutral current. This KPI is defined as the maximum neutral current in the network associated to the control strategy ζ for a given hourly scenario:

$$\mathbb{KPI}^{\zeta}_{\mathcal{I}_n,h} = \max_{ij} \left|\mathcal{I}_{ij,n,h}\right|. \quad (25)$$

  Note that for single-phase loads connected between the phase and the neutral wires, as usual in the European design of LV systems, neutral current appears in case of unbalance loads. Therefore, this KPI is a complementary measure of the network unbalance along with $\mathbb{KPI}^{\zeta}_{VUF0,h}$ and $\mathbb{KPI}^{\zeta}_{VUF2,h}$.

It is important to point out that the two first KPIs ($\mathbb{KPI}^{\zeta}_{loss}$ and $\mathbb{KPI}^{\zeta}_{viol}$) have a single value for an operation strategy ζ applied to a simulation scenario defined by σ, τ and ρ Conversely, the rest of the KPIs get different values for each analyzed hour h of the day.

TABLE 1. Performance of the optimization problem.

Parameter	**Bal. control** (*bal*)	**Unbal. control** (*unbal*)
# Constraints	572	566
# Variables	542	542
Average Time (ms)	277.8	201.4
Std. dev. Time (ms)	283.2	185.1
Percentile 95 Time (ms)	927.1	500.1

E. OPTIMIZATION PROBLEM IMPLEMENTATION

The two optimization problems for *bal* and *unbal* control strategies have been solved using an interior-point algorithm with ten randomly generated initialization points. The software was implemented using the *Python* library *pyomo* and the solver package *Ipopt* for large-scale nonlinear optimization problems. Some data associated to the performance of the optimization problem such as the size of the problem and the computational time taken to solve it are summarized in Table 1.

These results include all control strategies and scenario parameters variations in a hour-by-hour basis. The computational time has been obtained after 22320 executions of the optimization problem using an Intel i7, 8-core, 3.4 GHz, with 16 GB RAM and four parallel executions with 1 CPU core and 2 GB RAM per execution.

The balance control strategy involves a greater number of constraints because the equality equations among the phase powers injected by the PV inverters have to be enforced. This larger size of the resulting optimization problem implies a higher computational cost as shown the results in Table 1.

F. DAILY ANALYSIS

This section is devoted to analyze the performance of the proposed unbalanced control algorithm along the day with one-hour discretization. It is worth mentioning that the performance of the control strategies varies during the day. In particular, the load and generation profiles in Fig. 5 show

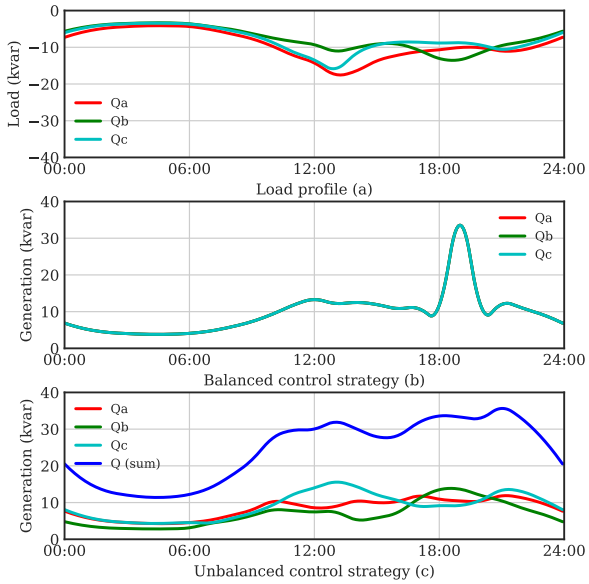

FIGURE 7. Daily evolution of (a) aggregated reactive power of loads, (b) aggregated reactive power of PV inverters for the *bal* strategy, (c) aggregated reactive power of PV inverters for the *unbal* strategy.

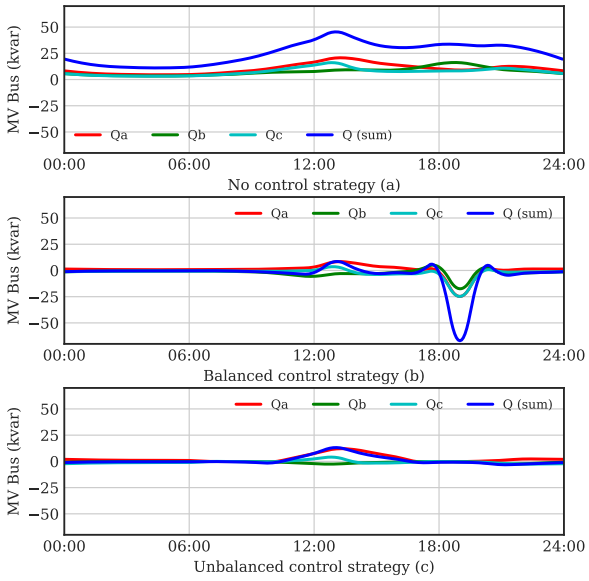

FIGURE 8. Daily evolution of the reactive power through the MV/LV transformer (a) *bc* strategy, (b) *bal* strategy, (c) *unbal* strategy.

the convenience of PV generation during sunshine hours, yet the impracticality during the night. This could be improved by the use of different energy sources or energy storage, such as EVs or BESSs.

In order to analyze how the control strategies performs on a daily basis, Fig. 6 shows the daily evolution of several relevant quantities for the following parameters' values: $\sigma = 1, \tau = 1, \rho = 1\ pu$. Additionally, Figs. 7 and 8 illustrate about the role that the balanced and the proposed unbalanced strategies plays in relation to the reactive power; the base case is operating at unity power factor so the reactive power setpoint of PV inverters is zero at every hour. Next comments arise from the analysis of all these figures:

- It is significant the voltage improvement achieved by the unbalance control strategy (see Fig.6.a), reducing notably the hourly network voltage range, mainly from 15:00 to 20:00 hours. This result is quite relevant if additional voltage control equipment were considered, like on load tap changers (OLTC) in secondary distribution transformers. Note that the unbalance control strategy would involve a wider action range of the OLTC control leading to an additional improvement in voltage levels and power losses.
- Fig.6.b shows as the proposed unbalance control strategy reduces the nodal voltage range by mainly raising the minimum voltages and, less significantly, lowering the maximum voltages. By contrast, the balance control strategy hardly affects the voltage evolution except the minimum voltages which are slightly higher than in the base case.
- Only the unbalance control strategy reduces significantly the neutral currents (as shown in Fig.6.c), achieving a reduction around 60%. The balance control strategy has hardly effect on neutral currents with regard to the base case as expected. Note that high neutral currents are strongly associated to unbalance situations which may lead to neutral wire break.
- Fig. 7.(a) presents the daily evolution of the aggregated load reactive power, while Figs. 7.(b) and 7.(c) show the total PV injected reactive power per phase for the balanced and unbalanced control strategies respectively. It is evident that the balanced control strategy requires higher reactive power injections than the proposed unbalance one, this difference being specially noticeable around 19:00 hours. Fig. 8 displays the injected reactive power from MV side of transformer for each of the three modes of operations. Once again, the new proposed unbalanced strategy proves to be the most efficient one because of minimizing the total reactive power demanded from the MV level, what in turns result on lower MV network power losses and an improved performance of secondary distribution transformers.

Note as the previous results are conclusive: it is more effective to use active power than reactive power as control variable to improve the LV network efficiency, being this result in line with the high R/X line ratios of these networks. These results not only makes evident this effect but additionally contributes to demonstrate the overall positive effect that the proposed unbalance power control has on the LV distribution network performance.

G. SENSITIVITY ANALYSIS

In order to analyze the effect of the scenario parameters on the control strategies' performance, a sensitivity analysis has been made showing the influence of each parameter (σ, τ and ρ) on the optimization results. The analysis is performed varying one parameter each, while the other two are

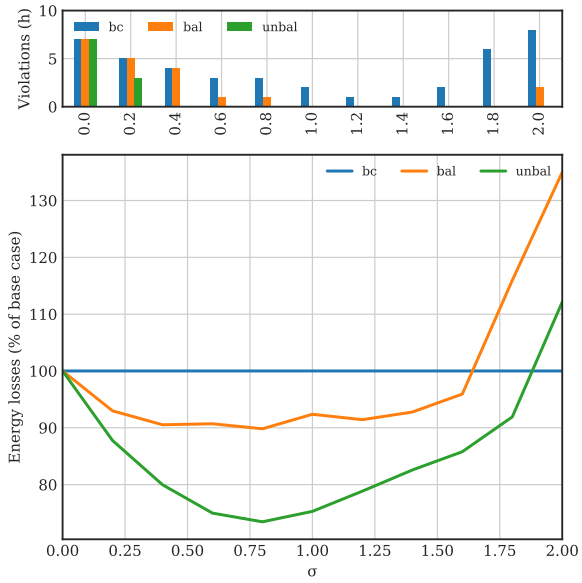

FIGURE 9. Sensitivity with respect to σ ($\tau = 1, \rho = 1$) of $\mathbb{KPI}^{\zeta}_{viol}$ and $\mathbb{KPI}^{\zeta}_{loss}$ for the different operation strategies.

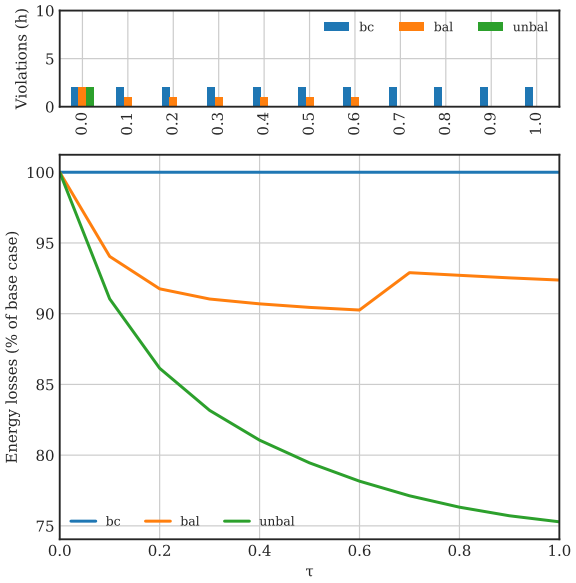

FIGURE 11. Sensitivity with respect to τ ($\sigma = 1, \rho = 1$) of $\mathbb{KPI}^{\zeta}_{viol}$ and $\mathbb{KPI}^{\zeta}_{loss}$ for the different operation strategies.

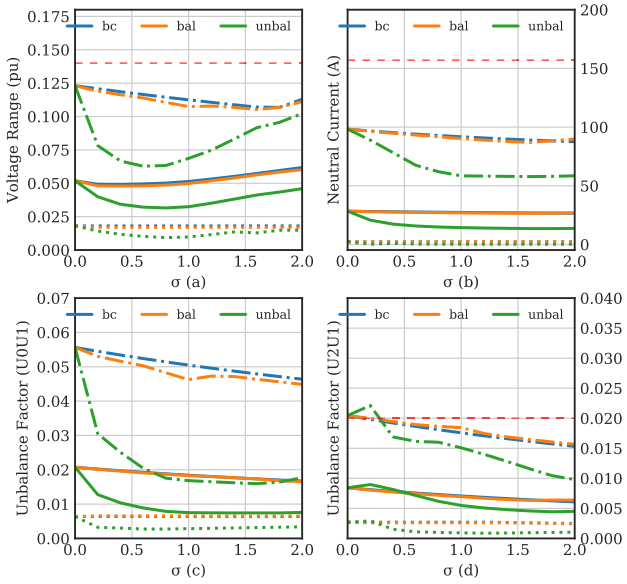

FIGURE 10. Sensitivity with respect to σ ($\tau = 1, \rho = 1$) of (a) $\mathbb{KPI}^{\zeta}_{\Delta V,h}$, (b) $\mathbb{KPI}^{\zeta}_{\mathcal{I}_n,h}$, (c) $\mathbb{KPI}^{\zeta}_{VUF0,h}$, (d) $\mathbb{KPI}^{\zeta}_{VUF2,h}$ for the different operation strategies. Maximum values (dash-dotted lined), average values (continous lines), minimum values (dotted lines).

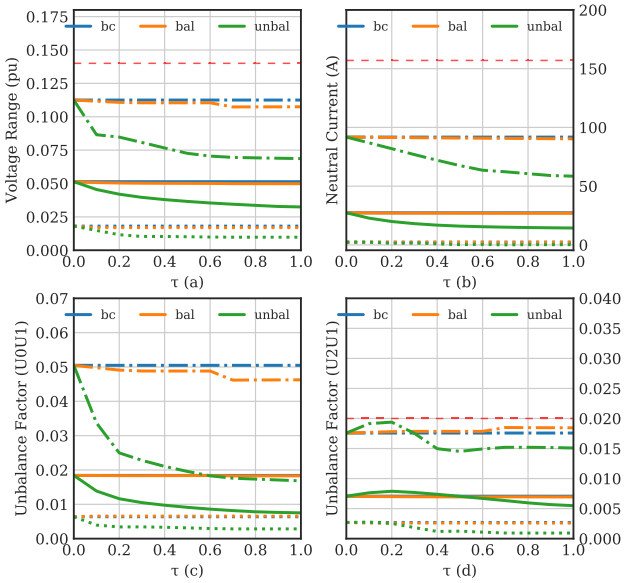

FIGURE 12. Sensitivity with respect to τ ($\sigma = 1, \rho = 1$) of (a) $\mathbb{KPI}^{\zeta}_{\Delta V,h}$, (b) $\mathbb{KPI}^{\zeta}_{\mathcal{I}_n,h}$, (c) $\mathbb{KPI}^{\zeta}_{VUF0,h}$, (d) $\mathbb{KPI}^{\zeta}_{VUF2,h}$ for the different operation strategies. Maximum values (dash-dotted lined), average values (continous lines), minimum values (dotted lines).

maintained constant to unit values. For each of the resulting simulation scenarios a 24-hour analysis similar to the one described in the previous subsection is carried out and the proposed KPIs are computed. In this sense, it is possible to directly represent the evolution of the two first KPIs ($\mathbb{KPI}^{\zeta}_{loss}$ and $\mathbb{KPI}^{\zeta}_{viol}$) as a function of the parameter that is modified. However, an alternative representation is required for the rest of the KPIs, because their dependency on the hour h. For this reason, the representation of these KPIs includes their maximum, average and minimum values to get a global idea of their behaviour. For conciseness purposes, only the most relevant comparisons are presented, but additional information can be obtained upon request or on the public project repository [51].

Firstly, regarding the parameter σ related to the PV generation penetration, the analysis of Figs. 9 and 10 reveals that:

- The proposed unbalanced control strategy eliminates all the voltage violations from $\sigma = 0.4\ pu$ which, otherwise, in case of applying a conventional strategy clearly increases with σ even in the case of optimal balanced control.

- The proposed unbalanced strategy reduces the power losses from the base case in a more efficient way than the classical balanced one. Firstly, it is achieved a losses reduction about 28% for $\sigma = 0.8\,pu$ which is much more than the 10% obtained by the classical balanced control. Secondly, it can be appreciated that an increase of losses with respect to the base case happens with higher values of σ and for any of the two control strategies. This is caused by the actions taken by PV inverters to enforce the regulatory voltage limits included in the optimization algorithm as shown in Fig. 9.(a). However, note that the increase of losses for the proposed unbalanced strategy is produced for a value of σ higher than that corresponding to the classical balanced control strategy. This implies that the new proposed control contributes on increasing the PV penetration levels more efficiently.
- In comparison with the unity power factor control, the unbalanced control strategy is the only one able to improve the network voltage range, neutral current and unbalanced KPIs significantly as shown in Fig. 10. It is surprisingly noting that the balance control strategy hardly improves the base case scenario as previously noticed with the daily analysis depicted in Fig. 7. The proposed unbalance control strategy is the most efficient one on not only reducing the average values of the KPIs but also narrowing the range between maximum and minimum values for all the KPIs and almost for any penetration level of PV generation σ.

Secondly, and regarding the parameter τ related to the proportion of PV generators with independent per-phase control capability, the analysis of Figs. 11 and 12 indicates that:

- The proposed unbalanced control strategy fixes all possible voltage violations from $\tau = 0.1\,pu$, unlike the balanced control that requires $\tau = 0.7\,pu$.
- The optimal performance occurs when all the three-phase distributed generators are equipped with the proposed independent per-phase control, $\tau = 1\,pu$, with an improvement of 25% on the technical losses.
- Similar to the analysis done for the PV generation penetration, σ parameter, the proposed unbalanced control strategy is the only one able to improve the voltage network range, neutral current and unbalanced factors significantly. Moreover, it can be clearly appreciated how all the KPIs improve when τ increases.

Finally, and regarding the influence of the oversizing parameter ρ, the proposed unbalance strategy performs much better than the balanced one for all the cases as shown in Fig. 13. In addition, it is quite interesting to remark that the KPI improvement with ρ is not as relevant as in the previous cases being almost constant for $\rho > 1.5\,pu$. This means that the PV inverter oversizing, related to the PV investment cost, is not a critical factor to consider because an excellent performance is achieved even without oversizing. This result is as expected because of the low influence of the PV reactive power injections, as previously analyzed.

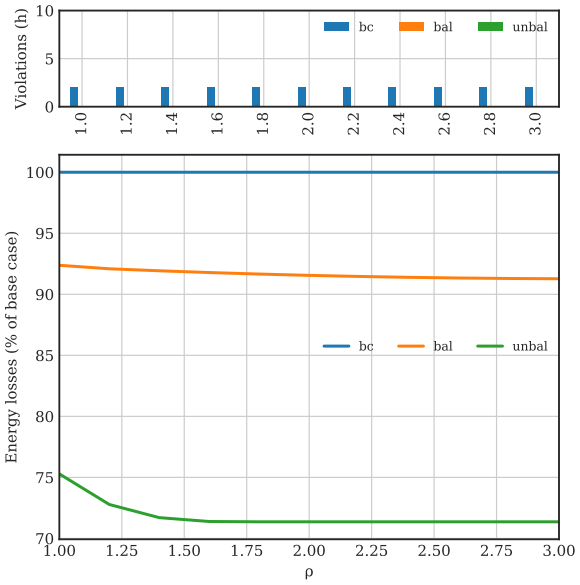

FIGURE 13. Sensitivity with respect to ρ ($\sigma = 1, \tau = 1$) of $\mathbb{KPI}^{\zeta}_{viol}$ and $\mathbb{KPI}^{\zeta}_{loss}$ for the different operation strategies.

V. CONCLUSION AND FUTURE WORK

This paper has explored the benefits of an independent per-phase control of DER inverters for minimizing the overall distribution network unbalance. For doing so, it has solved an optimization problem formulated to minimize the network active power losses considering a detailed three-phase four-wire network model. The paper has quantified the performance of the proposed operational strategy using the CIGRE Task Force C6.04.02 LV benchmark distribution network with different scenarios to evidence the influence of some key parameters as the DER penetration level, the percentage of independent per-phase DER inverters and the DER oversizing factor. In order to stress the benefits of the proposal, the results have been compared to those of two conventional operation strategies, namely unity power factor operation and optimal balance reactive power injection.

The results show that the proposed unbalance control strategy turns to be appreciably better than the conventional one based on balance reactive power injection, implying not only a noticeable reduction in power losses, unbalances and reactive power requirement from the MV network but also having a significant positive effect on voltage profiles. These results have been achieved by considering the new unbalanced control strategy on already existing three-phase inverters, being possible to conclude that the proposed control strategy allows to maximize the use of the current assets, deferring the need on new investments. Moreover, this new strategy is quite attractive to increase the DER penetration and the network loadability as long as three-phase four-wire generation units with independent per-phase control were integrated in the distribution network. This technical improvements can be reached without oversizing PV inverters. Due to the high R/X ratios of LV distribution networks it is more effective to manage unbalance active power injections than reactive

power. This result has important economic implications as the investment cost of the PV inverters is maintained.

Finally, it is important to remark that this strategy can be extended to new three-phase four-wire agents like EVs and BESSs to face the new challenges that LV distribution grids are going to experience in the near future. In the opinion of the authors, this work may have promising future extensions including, but not limited to, the unbalance operation of these new elements, the introduction of DER curtailment in the objective function and a multi-period formulation of the optimization problem. Moreover, the proposed formulation can be tailored along with advanced forecasting tools to develop real-time network control algorithms able to minimize the negative effects related to the uncertain and intermittent nature of PV generation, paving the way to a decarbonized power system.

REFERENCES

[1] H. Lee Willis, *Power Distribution Planning Reference Book*, 2nd ed. Boca Raton, FL, USA: CRC Press, 2004.

[2] A. Ghosh and G. Ledwich, *Power Quality Enhancement Using Custom Power Devices*. Norwell, MA, USA: Kluwer, 2002.

[3] T. A. Short, *Electric Power Distribution Handbook*. Boca Raton, FL, USA: CRC Press, 2004.

[4] S. M. Elnozahy and M. A. M. Salama, "A comprehensive study of the impacts of PHEVs on residential distribution networks," *IEEE Trans. Sustain. Energy*, vol. 5, no. 1, pp. 332–342, Jan. 2014.

[5] M. K. Gray and W. G. Morsi, "Power quality assessment in distribution systems embedded with plug-in hybrid and battery electric vehicles," *IEEE Trans. Power Syst.*, vol. 30, no. 2, pp. 663–671, Mar. 2015.

[6] J. Meyer, S. Hähle, P. Schegner, and C. Wald, "Impact of electrical car charging on unbalance in public low voltage grids," in *Proc. 11th Int. Conf. EPQU*, Lisbon, Portugal, Oct. 2011, pp. 1–6.

[7] C. Pansakul and K. Hongesombut, "Analysis of voltage unbalance due to rooftop PV in low voltage residential distribution system," in *Proc. Int. Congr. iEECON*, Chonburi, Thailand, Mar. 2014, pp. 1–4.

[8] S. Beharrysingh, "Phase unabalance on low-voltage electricity networks and its mitigation using static balancers," Ph.D. dissertation, Dept. Electron. Elect. Eng., Loughborough Univ., Leicestershire, U.K., Mar. 2014.

[9] R. Shaw, J. Simpson, D. Randles, T. Gozel, and L. N. Ochoa. (2014). *Deliverable 3.3 (Updated) Performance Evaluation of the Monitored LV Networks*. [Online]. Available: http://www.enwl.co.uk/docs/default-source/future-low-voltage/universityof-manchester-appendix-f.pdf

[10] S. Lu, S. Repo, D. D. Giustina, F. A. C. Figuerola, A. Löf, and M. Pikkarainen, "Real-time low voltage network monitoring—ICT architecture and field test experience," *IEEE Trans. Smart Grid*, vol. 6, no. 4, pp. 2002–2012, Jul. 2015.

[11] S. Weckx, C. G. de Miguel, P. Vingerhoets, and J. Driesden, "Phase switching and phase balancing to cope with a massive photovoltaic penetration," in *Proc. Int. Conf. CIRED*, Stockholm, Sweden, Jun. 2013, pp. 1–4.

[12] P. K. C. Wong, A. Kalam, and R. Barr, "Modelling and analysis of practical options to improve the osting capacity of low voltage networks for embedded photo-voltaic generation," *IET Renew. Power Gener.*, vol. 11, no. 5, pp. 625–632, 2017.

[13] *TEC Static Balancers*. Accessed: Feb. 20, 2019. [Online]. Available: http://www.claudelyons.co.uk/products/transformers?id=139

[14] F. Shahnia, P. Wolfs, and A. Ghosh, "Voltage unbalance reduction in low voltage feeders by dynamic switching of residential customers among three phases," in *Proc. IEEE Power Energy Soc. Gen. Meeting*, Vancouver, BC, Canada, Jul. 2013, pp. 1–5.

[15] W. M. Siti, A. Jimoh, and D. Nicolae, "Distribution network phase load balancing as a combinatorial optimization problem using fuzzy logic and Newton raphson," *Electr. Power Syst. Res.*, vol. 81, no. 5, pp. 1079–1087, 2011.

[16] H. Beltran, N. Aparicio, E. Belenguer, and C. C. García, "Fuel cell connection inverters used for unbalance compensation in low voltage distribution systems," in *Proc. Int Conf. ICREPQ*, Santander, Spain, Mar. 2008, pp. 1–8.

[17] B. Meersman, B. Renders, L. Degroote, T. Vandoorn, and L. Vandevelde, "Three-phase inverter-connected DG-units and voltage unbalance," *Electr. Power Syst. Res.*, vol. 81, no. 4, pp. 899–906, 2011.

[18] R. Caldon, M. Coppo, and R. Turri, "Voltage unbalance compensation in LV networks with inverter interfaced distributed energy resources," in *Proc. IEEE Int. Energy Conf. Exhib. (ENERGYCON)*, Florence, Italy, Sep. 2012, pp. 527–532.

[19] F. Geth, J. Tant, R. Belmans, and J. Driesen, "Balanced and unbalanced inverter strategies in battery storage systems for low-voltage grid support," *IET Gener., Transmiss. Distrib.*, vol. 9, no. 10, pp. 929–936, Sep. 2015.

[20] S. Weckx and J. Driesen, "Load balancing with EV chargers and PV inverters in unbalanced distribution grids," *IEEE Trans. Sustain. Energy*, vol. 6, no. 2, pp. 635–643, Apr. 2015.

[21] B. Meersman, B. Renders, L. Degroote, T. Vandoorn, and L. Vandevelde, "The influence of grid-connected three-phase inverters on voltage unbalance," in *Proc. IEEE Power Energy Soc. Gen. Meeting*, Providence, RI, USA, Jul. 2013, pp. 1–9.

[22] *Current and Future Cost of Photovoltaics. Long-Term Scenarios for Market Development, System Prices and LCOE of Utility-Scale PV Systems*, Study Behalf Agora Energiewend, Fraunhofer-Inst. Sol. Energy Syst., Freiburg im Breisgau, Germany, Feb. 2015.

[23] K. Turitsyn, P. Šulc, S. Backhaus, and M. Chertkov, "Distributed control of reactive power flow in a radial distribution circuit with high photovoltaic penetration," in *Proc. IEEE Power Energy Soc. Gen. Meeting*, Providence, RI, USA, Jul. 2013, pp. 1–6.

[24] B. Bletterie, S. Kadam, A. Zegers, and Z. Z. Miletic, "On the effectiveness of voltage control with PV inverters in unbalanced low voltage networks," in *Proc. Int. Conf. CIRED*, Lyon, France, Jun. 2015, pp. 1–55, Paper 1082.

[25] F. Shahnia, R. Majumder, A. Ghosh, G. Ledwich, and F. Zare, "Voltage imbalance analysis in residential low voltage distribution networks with rooftop PVs," *Electr. Power Syst. Res.*, vol. 81, no. 9, pp. 1805–1814, 2011.

[26] E. Dall'Anese, S. V. Dhople, and G. B. Giannakis, "Optimal dispatch of photovoltaic inverters in residential distribution systems," *IEEE Trans. Sustain. Energy*, vol. 5, no. 2, pp. 487–497, Apr. 2014.

[27] P. Šulc, S. Backhaus, and M. Chertkov, "Optimal distributed control of reactive power via the alternating direction method of multipliers," *IEEE Trans. Energy Convers.*, vol. 29, no. 4, pp. 968–977, Dec. 2014.

[28] E. Demirok, P. C. González, K. H. B. Frederiksen, D. Sera, P. Rodriguez, and R. Teodorescu, "Local reactive power control methods for overvoltage prevention of distributed solar inverters in low-voltage grids," *IEEE J. Photovolt.*, vol. 1, no. 2, pp. 174–182, Oct. 2011.

[29] P. Jahangiri and D. C. Aliprantis, "Distributed Volt/VAr control by PV inverters," *IEEE Trans. Power Syst.*, vol. 28, no. 3, pp. 3429–3439, Aug. 2013.

[30] X. Su, M. A. S. Masoum, and P. J. Wolfs, "Optimal PV inverter reactive power control and real power curtailment to improve performance of unbalanced four-wire LV distribution networks," *IEEE Trans. Sust. Energy*, vol. 5, no. 3, pp. 967–977, Jul. 2014.

[31] *Benchmark Systems for Network Integration of Renewable and Distributed Energy Resources*, document TF C6.04.02, CIGRE, 2013.

[32] M. S. Chen and W. E. Dillon, "Power system modelling," *Proc. IEEE*, vol. 62, no. 7, pp. 901–915, Jul. 1974.

[33] J. Arrillaga and C. P. Arnold, *Computer Analysis of Power Systems*. Hoboken, NJ, USA: Wiley, 1994.

[34] D. E. Rodas, A. Padilha-Feltrin, and L. F. Ochoa, "Distribution transformers modeling with angular displacement—Actual values and per unit analysis," *Revista Controle Automaca*, vol. 18, no. 4, pp. 490–500, 2007.

[35] M. A. Laughton, "Analysis of unbalanced polyphase networks by the method of phase co-ordinates. Part 1: System representation in phase frame of reference," *Proc. Inst. Electr. Eng.*, vol. 115, no. 8, pp. 1163–1172, 1968.

[36] D. Pudjianto, P. Djapic, D. S. Papadaskalopoulos, S. Giannelos, and G. Strbac. *Monitoring & Impact Assessment of Project Demonstrations. D8.6 Report About System Wide Benefits of UPGRID Services*. Accessed: Jul. 17, 2019. [Online]. Available: http://upgrid.eu/wp-content/uploads/2018/01/UPGRID_WP8_D8_6_System_wide_benefits_v05_Final.pdf

[37] W. H. Kersting and W. H. Phillips, "Distribution feeder line models," *IEEE Trans. Ind. Appl.*, vol. 31, no. 4, pp. 715–720, Jul. 1995.

[38] L. Moreno-Díaz, E. Romero-Ramos, A. Gómez-Expósito, E. Cordero-Herrera, J. R. Rivero, and J. S. Cifuentes, "Accuracy of electrical feeder models for distribution systems analysis," in *Proc. Int. Conf. SEST*, Seville, Spain, 2018, pp. 1–6.

[39] M. H. Haque, "Load flow solution of distribution systems with voltage dependent load models," *Electr. Power Syst. Res.*, vol. 36, no. 3, pp. 151–156, 1996.
[40] B. Bletterie, A. Latif, P. Zehetbauer, S. Martínez Villanueva, E. Romero-Ramos, and H. Renner, "On the impact of load modelling on distribution network studies," in *Proc. Eur. IEEE ISGT*, Turin, Italy, Sep. 2017, pp. 1–6, Paper 1245.
[41] B. Meersman, B. Renders, L. Degroote, T. Vandoorn, J. De Kooning, and L. Vandevelde, "Overview of three-phase inverter topologies for distributed generation purposes," in *Proc. Int. Conf. i-SUP*, Bruges, Belgium, Apr. 2010, pp. 24–28.
[42] P. Verdelho and G. D. Marques, "Four-wire current-regulated PWM voltage converter," *IEEE Trans. Ind. Electron.*, vol. 45, no. 5, pp. 761–770, Oct. 1998.
[43] J. Liang, T. C. Green, C. Feng, and G. Weiss, "Increasing voltage utilization in split-link four-wire inverters," *IEEE Trans. Power Electron.*, vol. 24, no. 6, pp. 1562–1569, Jun. 2009.
[44] J. M. Carrasco, L. G. Franquelo, J. T. Bialasiewicz, E. Galvan, R. C. PortilloGuisado, M. A. M. Prats, J. I. Leon, and N. Moreno-Alfonso, "Power-electronic systems for the grid integration of renewable energy sources: A survey," *IEEE Trans. Ind. Electron.*, vol. 53, no. 4, pp. 1002–1016, Jun. 2006.
[45] T. Beach, A. Kozinda, and V. Rao. *Advances Inverters for Distributed PV: Latent Opportunities for Localized Reactive Power Compensation*. Cal X Clean Coalition Energy C226. Accessed: May 4, 2014. [Online]. Available: http://www.clean-coalition.org/site/wp-content/uploads/2013/10/CC_PV_AI_Paper_Final_Draft_v2.5_05_13_2013_AK.pdf
[46] S. Vlachopoulos and C. Demoulias, "Voltage regulation in low-voltage rural feeders with distributed PV systems," in *Proc. Int. Conf. IEEE EUROCON*, Lisbon, Portugal, Apr. 2011, pp. 1–4.
[47] F. Capitanescu, M. Glavic, D. Ernst, and L. Wehenkel, "Interior-point based algorithms for the solution of optimal power flow problems," *Electr. Power Syst. Res.*, vol. 77, nos. 5–6, pp. 508–517, 2007.
[48] A. Wächter and L. T. Biegler, "On the implementation of a primal-dual interior point filter line search algorithm for large-scale nonlinear programming," *Math. Program.*, vol. 106, no. 1, pp. 25–57, 2006.
[49] *Regulation of the Activities of Transmission, Distribution, Retail, Supply and Authorization Procedures of Electrical Installations*, Ministry Economy Bus., Madrid, Spain, 2000.
[50] *Voltage Characteristic of Electricity Supplied by Public Distribution Systems*, document EN 50160, 2011.
[51] A. Gastalver-Rubio, E. Romero-Ramos, and J. M. Maza-Ortega, "Improving the performance of low voltage networks by an optimized unbalance operation of three-phase distributed generators," *IEEE DataPort*. Accessed: Nov. 14, 2019, doi: 10.21227/d176-x951.

ADOLFO GASTALVER-RUBIO received the B.E. and M.E. degrees in computer science and engineering, and the M.Sc. degree in electrical engineering from the University of Seville, Seville, Spain, in 2012, 2013, and 2017, respectively. He is currently pursuing the Ph.D. degree in electrical engineering with the University of Seville. In 2013, he joined Ingelectus SL, Seville, Spain, as a CS Engineer and a CIO. His works focus on renewable energy integration, and the application of artificial intelligence and optimization techniques in low voltage electrical power systems.

ESTHER ROMERO-RAMOS received the Electrical Engineering and Ph.D. degrees from the University of Seville, Seville, Spain, in 1992 and 1999, respectively. Since 1993, she has been with the Department of Electrical Engineering, University of Seville, where she is currently a Full Professor. She is interested in state estimation, load flow problems, optimal power system operation and analysis, and control of active distribution systems.

JOSÉ MARÍA MAZA-ORTEGA received the Electrical Engineering and Ph.D. degrees from the University of Seville, Seville, Spain, in 1996 and 2001, respectively. Since 1997, he has been with the Department of Electrical Engineering, University of Seville, where he is currently an Associate Professor. His primary areas of interest are power quality, harmonic filters, integration of renewable energies, and power electronics.